Applied Surface Science 256 (2010) 6153–6156

Contents lists available at ScienceDirect

Applied Surface Science

journal homepage: www.elsevier.com/locate/apsusc

Improved ultraviolet/visible rejection ratio using $MgZnO/SiO_2$/n-Si heterojunction photodetectors

Da-Yong Jiang[a], Xi-Yan Zhang[a,*], Quan-Sheng Liu[a], Zhao-Hui Bai[a], Li-Ping Lu[a], Xiao-Chun Wang[a], Xiao-Yun Mi[a], Neng-Li Wang[a], De-Zhen Shen[b]

[a] School of Materials Science and Engineering, Changchun University of Science and Technology, Changchun 130022, China
[b] Key Laboratory of Excited State Processes, Changchun Institute of Optics, Fine Mechanics and Physics, Chinese Academy of Sciences, Changchun 130033, China

ARTICLE INFO

Article history:
Received 26 January 2010
Received in revised form 6 March 2010
Accepted 6 March 2010
Available online 15 March 2010

Keywords:
MgZnO
Photodetector
Heterojunction
Ultraviolet/visible rejection ratio

ABSTRACT

We report on the fabrication and characterization of $MgZnO/SiO_2$/n-Si structured photodetectors, for the visible–blind monitoring. The current–voltage curve of the heterojunction shows obvious rectifying behaviors. In the visible range, the photocurrent decreased rapidly. In additionally, the ultraviolet/visible rejection ratio (R340 nm/R500 nm) was about four orders of magnitude at reverse bias, indicating a high degree of visible blindness. The key role of the insulating SiO_2 layer will be discussed in terms of the band diagrams of the heterojunctions.

Published by Elsevier B.V.

1. Introduction

Wide band gap materials have received much attention for their potential application in various optoelectronic devices. For example, ZnO/MgZnO material system is well suited as a photodetector material operating in the ultraviolet (UV) region [1–6]. ZnO and MgZnO also possess unique figures of merit, such as availability of lattice-matched single-crystal substrates (ZnO and MgO for hexagonal and cubic MgZnO films, respectively) [7], tunable band gap energy (3.3–7.8 eV) [8–10], relatively low thin-film growth temperatures (373–1023 K) [10], and radiation hardness [11], etc. A number of reports on photoconductive, MSM, and *p*–*n* junction UV detectors have been reported in the literature [2,12,13]. While the vast majority of these photodetectors were fabricated from films grown on sapphire substrates [5,7], and only a few utilized on Si as the substrate [8]. Nevertheless, the use of silicon offers many benefits, such as large area, low-cost, highly perfect substrates are readily available, a very sophisticated backside process technology has been developed over many years, and thermal expansion mismatch between detector arrays and read-out electronics would be mitigated.

In most UV detection applications, it is both important and necessary to achieve devices with large UV/visible rejection ratio. ZnO/Si structured photodetectors have been successfully demonstrated by a few researchers [14–16]. However, it is noteworthy that the quantity defined as ratios of photoresponse at 380–500 nm are all less than 1. In this letter, $MgZnO/SiO_2$/n-Si structured photodetectors have been fabricated and obtained high UV/visible (340 nm/500 nm) rejection ratio. Meanwhile, we have also discussed the behavior of SiO_2 layer, which can reduce the dark current and enhance the UV/visible rejection ratio.

2. Experiments

The sample used in this study was grown by radio-frequency (RF) magnetron sputtering technique. An $Mg_{0.05}Zn_{0.95}O$ target was prepared by sintering mixture of 99.99% pure MgO and ZnO powders at 1273 K for 10 h in air ambient. Before deposition, the n-type Si(1 1 1) substrate was covered with a 10 nm SiO_2 layer of rapid thermal oxidation. The chamber was pumped down to a high vacuum of 10^{-4} Pa before introducing Ar sputtering gas. The working pressure in the chamber was kept at 1 Pa with RF power of 150 W and the substrate temperature was controlled at about 773 K. Ni/Au and In metals were deposited using vacuum evaporation as MgZnO and Si contacts, respectively. In order to obtain good ohmic contacts, the metalized devices were then thermally annealed in vacuum at 573 K.

X-ray diffraction (XRD) spectra were collected with a D/max-RA X-ray spectrometer (Rigaku International Corp., Japan) with CuKα radiation of 1.543 Å to obtain the structural information of the film.

* Corresponding author. Tel.: +86 431 85583016; fax: +86 431 85583015.
E-mail address: xiyzhang@126.com (X.-Y. Zhang).

0169-4332/$ – see front matter. Published by Elsevier B.V.
doi:10.1016/j.apsusc.2010.03.051

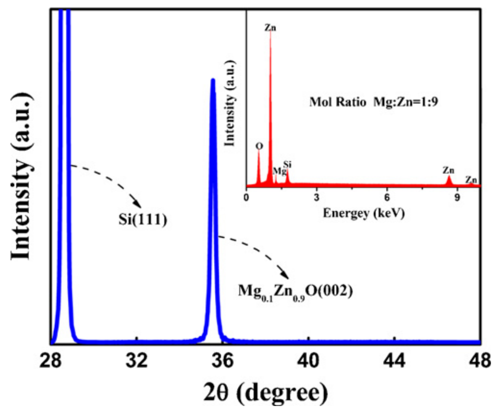

Fig. 1. XRD spectra of the MgZnO thin-film prepared on the SiO_2/n-Si substrate by RF magnetron sputtering technique. The inset shows the EDS data for the MgZnO thin film.

A Hatachi S4800 energy dispersive spectroscopy (EDS) was used to determine the Mg/Zn ratio in the films. The surface morphology was observed by using a DI 3100 atomic force microscopy (AFM). The typical current–voltage (*I–V*) characteristics of the photodetectors were measured by a semiconductor analyzer (Keithley 4200). The spectral responsivity was measured with a standard lock-in amplifier, where a 150 W Xe lamp was used as the light source.

3. Results and discussion

Fig. 1 shows the XRD pattern of MgZnO thin-film grown on the SiO_2/n-Si(1 1 1) substrate. The appearance of only the (0 0 2) diffraction peak indicated that the film is highly *c*-axis oriented and corresponds to the hexagonal wurtzite structure of MgZnO. The composition of the film was measured by EDS and obtained to be $Mg_{0.1}Zn_{0.9}O$, as shown in the inset of Fig. 1. The surface morphology of the $Mg_{0.1}Zn_{0.9}O$ film was observed by using AFM under normal air condition. Fig. 2(a) shows a microstructure with the crystallite size ranging from 27 to 45 nm, implying that the grains are uniform. Fig. 2(b) is the stereoscopic model of the film. The value of the root mean square (RMS) is only 2.1 nm, indicating that the film is rather smooth, and it is reasonable to believe that the crystal quality is good.

I–V characteristics of the heterojunction photodetectors in dark are shown in Fig. 3(a). The upper left inset shows the *I–V* curve of the $Mg_{0.1}Zn_{0.9}O$/n-Si device without illumination. The $Mg_{0.1}Zn_{0.9}O/SiO_2$/n-Si structured photodetector shows a good rectifying characteristic with low dark current, 10 nA at 5 V bias. Compared with $Mg_{0.1}Zn_{0.9}O$/n-Si, the $Mg_{0.1}Zn_{0.9}O/SiO_2$/n-Si photodetector has lower dark current obviously. Fig. 3(b) shows *I–V* plots from Ni/Au-$Mg_{0.1}Zn_{0.9}O$ and In-Si contacts. The linear trend shows good ohmic contacts, implying that the rectifying behavior originates from the heterojunction.

Fig. 4(a) presents the responsivity as a function of wavelength for the $Mg_{0.10}Zn_{0.90}O/SiO_2$/n-Si photodetector at zero bias. The incident optical power was measured with a calibrated UV-enhanced Si photodetector. Because there will generate a built-in electric field in the heterojunction, which can be confirmed by the rectifying characteristic of the *I–V* curve. Therefore, the photogenerated carriers will be sweep out by the electric field. In the UV spectral region, the responsivity of the photodetector had a little decrease from 340 to 300 nm. The peak photoresponse was found at 340 nm with the responsivity of 0.20 A/W.

The most important improvement of our devices is the higher UV/visible rejection ratio than the reported results [14–17]. The reported ZnO/Si photodetectors remain an obvious photoresponse to visible light, which would limit its direct application in UV detection under a visible light background. The normalized photoresponse spectrum of $Mg_{0.10}Zn_{0.90}O/SiO_2$/n-Si photodetector at reverse bias of −2 V was shown in Fig. 4(b). The spectra of $Mg_{0.10}Zn_{0.90}O$/n-Si device were also presented for comparison. The UV/visible rejection ratio was only one order of magnitude. The photodetector with SiO_2 insulator has lower response in the visible range, in other words, this type photodetector has larger UV/visible rejection ratio (R340 nm/R500 nm), which is about four orders of magnitude, indicating a high degree of visible blindness. It should be noted that the SiO_2 insulator will play a key role in the photoresponse.

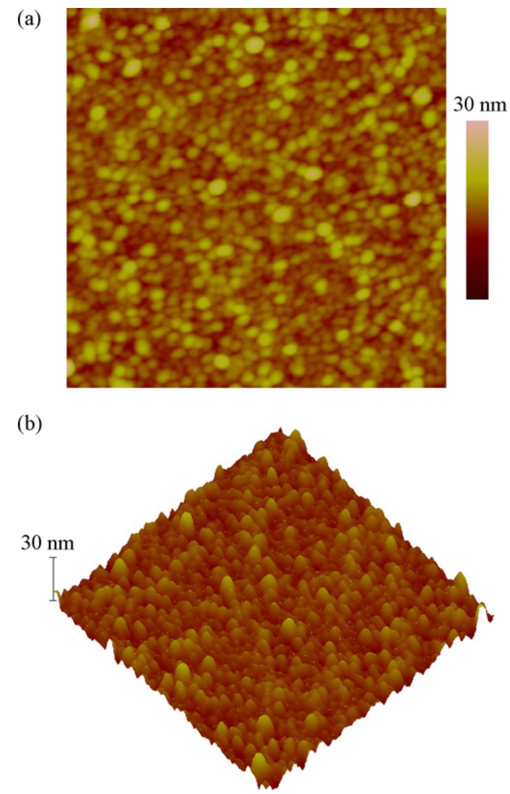

Fig. 2. (a) A topography of the $Mg_{0.1}Zn_{0.9}O$ thin film. (b) A stereoscopic profile of the topography. The scan size is 1 μm × 1 μm.

In order to well understand the principle of the $MgZnO/SiO_2$/n-Si photodetector, the energy band diagram of this heterojunction derived from Anderson model [18] is drawn in Fig. 5(a). According to the values of electron affinity energy as well as the band gap of Si and MgZnO, it is derived that the valence band offset ΔE_V is much larger than the conduction band offset ΔE_C. Moreover, it should be noted that the depletion region of SiO_2 insulator within the heterojunction is critical for the carrier transport.

To further demonstrate the key role of the insulator SiO_2 layer in visible–blind UV detecting, the energy band diagrams of MgZnO/n-Si and $MgZnO/SiO_2$/n-Si structures were displayed in Fig. 5(b) and (c), respectively. As can be seen from Fig. 5(b), a visible light arriving at the junction will pass through the MgZnO layer and be absorbed in the underlying Si to generate *e–h* pairs. These photogenerated holes will drift toward MgZnO side driven by the applied bias. However, the absorption of ultraviolet photons will take place in the MgZnO layer, and the photogenerated electrons will be swept to the Si region. If there is a SiO_2 insulator in the junction, the transport situation will change. In this case, the insulator will easily block the movement of the holes. That is the reason why no response was observed when illuminating visible light. Although the insulator may also block the electrons when an UV light irradiates, the much larger tunneling probability for electrons makes the heterojunction

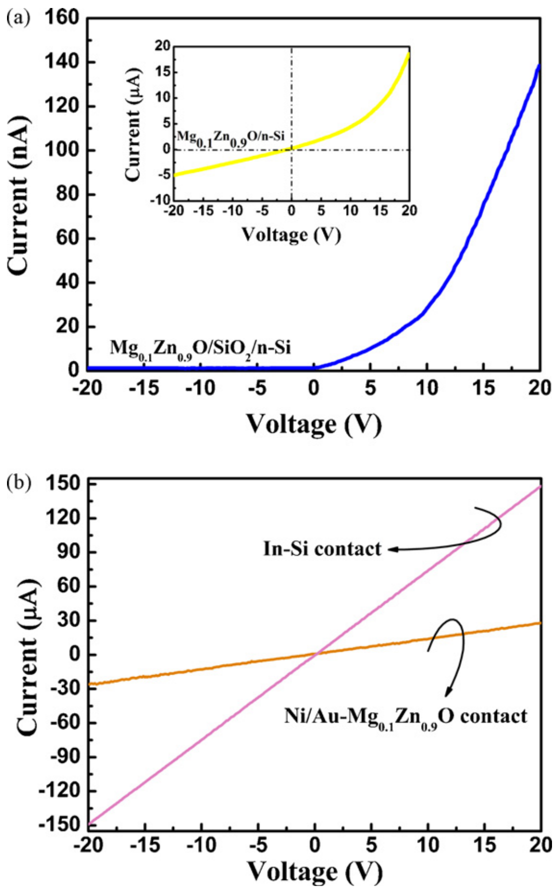

Fig. 3. (a) Dark current of the $Mg_{0.1}Zn_{0.9}O/SiO_2$/n-Si photodetector as a function of the bias voltage, and the inset shows the *I–V* curve of the $Mg_{0.1}Zn_{0.9}O$/n-Si photodetector without illumination. (b) Ni/Au-$Mg_{0.1}Zn_{0.9}O$ and In-Si ohmic contacts.

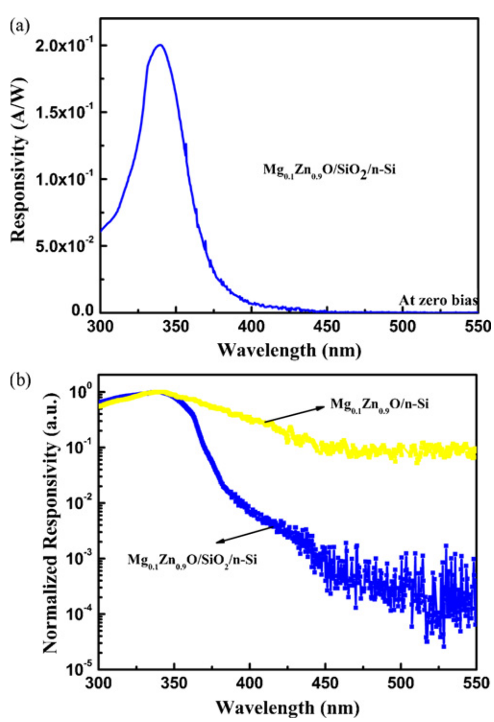

Fig. 4. (a) Spectral photoresponse measured from the $Mg_{0.1}Zn_{0.9}O/SiO_2$/n-Si photodetector at zero bias. (b) Normalized photoresponse spectrum of photodetectors based on $Mg_{0.1}Zn_{0.9}O/SiO_2$/n-Si and $Mg_{0.1}Zn_{0.9}O$/n-Si heterojunctions at reverse bias.

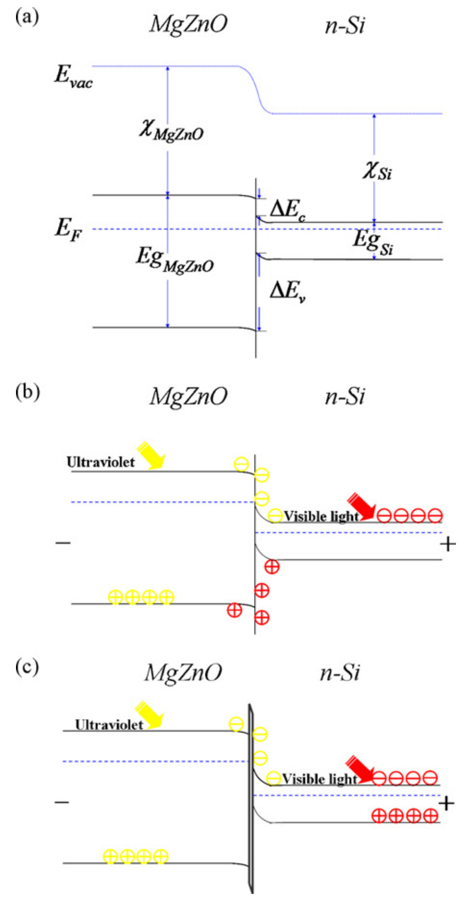

Fig. 5. Schematic energy band diagrams of (a) MgZnO/n-Si at zero bias, (b) MgZnO/n-Si at reverse bias, and (c) $MgZnO/SiO_2$/n-Si at reverse bias, respectively.

with good photoresponse, seeing the drawing of Fig. 5(c). Hence, the insulator will result in enhancing the UV/visible rejection ratio.

4. Conclusions

In summary, a visible–blind photodetector based on the heterojunction of $Mg_{0.1}Zn_{0.9}O/SiO_2$/n-Si has been fabricated and characterized by photoresponse spectrum. The peak responsivity of the device was 0.2 A/W at zero bias. The most important improvement of our photodetector is the larger UV/visible rejection ratio in comparison with the $Mg_{0.1}Zn_{0.9}O$/n-Si structured photodetector. The UV/visible rejection ratio was enlarged from one to four orders of magnitude. The SiO_2 insulator displayed a strong influence on the response in the visible range, and the physical mechanism is that the photogenerated holes in Si region can be easily blocked by the insulator. We believe that these results represent a significant step toward achieving high UV/visible rejection ratio for the UV photodetector.

Acknowledgement

This work is supported by the National Natural Science Foundation of China under Grant No. 50772016.

References

[1] S. Liang, H. Shen, Y. Liu, Z. Huo, Y. Lu, H. Shen, J. Cryst. Growth 225 (2001) 110.
[2] W. Yang, R.D. Vispute, S. Choopun, R.P. Sharma, T. Venkatesan, H. Shen, Appl. Phys. Lett. 78 (2001) 2707.
[3] W. Yang, S.S. Hullavarad, B. Nagaraj, I. Takeuchi, R.P. Sharma, T. Venkatesan, R.D. Vispute, H. Shen, Appl. Phys. Lett. 82 (2003) 3424.

[4] J.B.K. Law, J.T.L. Tong, Appl. Phys. Lett. 88 (2006) 133114.
[5] C.Y. Lu, S.J. Chang, S.P. Chang, C.T. Lee, C.F. Kuo, H.M. Chang, Appl. Phys. Lett. 89 (2006) 153101.
[6] Y. Vygranenko, K. Wang, A. Nathan, Appl. Phys. Lett. 89 (2006) 172105.
[7] S.S. Hullavarad, S. Dhar, B. Varughese, I. Takeuchi, T. Venkatesan, R.D. Vispute, J. Vac. Sci. Technol. A 23 (2005) 982.
[8] J. Narayan, A.K. Sharma, A. Kvit, C. Jin, J.F. Muth, O.W. Holland, Solid State Commun. 121 (2002) 9.
[9] S. Kumar, V. Gupte, K. Sreenivas, J. Phys. Condens. Matter 18 (2006) 3343.
[10] S. Choopun, R.D. Vispute, W. Yang, R.P. Sharma, T. Venkatesan, H. Shen, Appl. Phys. Lett. 80 (2002) 1529.
[11] F.D. Auret, S.A. Goodman, M. Hayes, M.J. Legodi, H.A. van Laarhoven, D.C. Look, Appl. Phys. Lett. 79 (2001) 3074.
[12] D.Y. Jiang, J.Y. Zhang, K.W. Liu, Y.M. Zhao, C.X. Cong, Y.M. Lu, B. Yao, Z.Z. Zhang, D.Z. Shen, Semicond. Sci. Technol. 22 (2007) 687.
[13] K.W. Liu, D.Z. Shen, C.X. Shan, J.Y. Zhang, B. Yao, D.X. Zhao, Y.M. Lu, X.W. Fan, Appl. Phys. Lett. 91 (2007) 201106.
[14] I.S. Jeong, J.H. Kim, S. Im, Appl. Phys. Lett. 83 (2003) 2946.
[15] R.A. Ismail, Ala Al-Naimi, A.A. Al-Ani, Semicond. Sci. Technol. 23 (2008) 075030.
[16] C.H. Park, I.S. Jeong, J.H. Kim, S. Im, Appl. Phys. Lett. 82 (2003) 3973.
[17] K. Koike, K. Hama, I. Nakashima, G.Y. Takada, K.I. Ogata, S. Sasa, M. Inoue, M. Yano, J. Cryst. Growth 278 (2005) 288.
[18] S.M. Sze, Physics of Semiconductor Devices, 2nd ed., Wiley, New York, 1981.